JEBAT, 2025, Vol 8, No 1, 59-68
https://doi.org/10.54987/jebat.v8i1.1126

Mathematical Modelling of Zinc-Induced Inhibition on Fermentative Biohydrogen Production by Granular Sludge

Mohd Izuan Effendi Halmi[1] and Mohd Yunus Shukor[2]*

[1]Department of Land Management, Faculty of Agriculture, Universiti Putra Malaysia, 43400 UPM Serdang, Selangor, Malaysia.
[2]Department of Biochemistry, Faculty of Biotechnology and Biomolecular Sciences, Universiti Putra Malaysia, UPM 43400 Serdang, Selangor, Malaysia.

*Corresponding author:
Mohd Yunus Shukor
Department of Biochemistry,
Faculty of Biotechnology and Biomolecular Sciences,
Universiti Putra Malaysia,
UPM 43400 Serdang,
Selangor,
Malaysia.
Email: mohdyunus@upm.edu.my

HISTORY

Received: 14th May 2025
Received in revised form: 15th July 2025
Accepted: 29th July 2025

KEYWORDS

Biohydrogen
Anaerobic granular sludge
Predictive models
MOORA
MMF model

ABSTRACT

Biohydrogen production in anaerobic granular sludge reactors has led to the development of stable microbial communities that enhance substrate conversion rates. The fermentation process of sucrose by these microbial communities is a sustainable approach to hydrogen production, making biological dark fermentation an effective method for renewable biohydrogen generation. This study analyzed biohydrogen production data from granular sludge in a packed-bed upflow reactor processing sucrose-containing wastewater at 26 °C for more than 500 days, using multiple predictive kinetic models. The biohydrogen production data were converted to natural logarithms to improve linearity and reduce variance. The Morgan–Mercer–Flodin (MMF) model, coupled with the Multi-Objective Optimization by Ratio Analysis (MOORA) approach, achieved the best statistical results among nine tested predictive models based on error functions, including the highest adjusted R^2 value and the lowest RMSE, AICc, BIC, and HQC values. The MMF model successfully predicted all stages of hydrogen production sigmoidal growth while also modeling zinc-induced stimulation and inhibition effects. The combination of multi-criteria analysis (MOORA) with classical error-function analyses improved model discrimination, enabling a deeper understanding of microbial growth patterns under different environmental conditions to optimize biohydrogen production systems.

INTRODUCTION

Biohydrogen production is touted as a promising solution to sustainable energy needs because it simultaneously enables cleaner power generation and waste elimination. In biohydrogen production, microorganisms convert different organic materials into hydrogen through their metabolic activities [1,2]. The biotechnological method is gaining popularity because it aligns with global efforts to establish carbon-neutral energy systems and clean up environmental contamination [3]. Biohydrogen production occurs through dark fermentation, photofermentation, and biophotolysis, each of which depends on distinct microbial communities. The main microorganisms used in dark fermentation studies include anaerobic bacteria from *Clostridium* spp., *Thermoanaerobacterium* spp., *Enterobacter* spp., and *Caldicellulosiruptor* spp., as well as diverse microbial communities [4–7]. These microorganisms can metabolize simple sugars and complex compounds into hydrogen gas while simultaneously generating organic acids and alcohols through fermentation [8,9].

Photofermentation in purple nonsulfur photosynthetic bacteria, including *Rhodobacter sphaeroides* and *Rhodopseudomonas palustris*, converts organic acids into hydrogen gas, achieving higher substrate-based hydrogen yields. These organisms use light energy but exhibit increased sensitivity to environmental changes, and research applications remain limited due to engineering constraints [10]. In another route, the water biophotolysis process for microalgae that produce hydrogen gas occurs under specific light exposure but is tightly linked to strict management of several interrelated factors, including substrate choice, temperature, pH levels, nutrient supply, and good reactor design.

The production of fermentative hydrogen from agricultural waste benefits most from carbohydrate-based substrates, including glucose, xylose, and hydrolysates, which offer excellent biodegradability and stable conversion rates [11,12]. The hydrogen production rate depends heavily on temperature because both mesophilic (30–40 °C) and thermophilic (50–80

°C) ranges are commonly used. *Thermotoga* spp. and *Caldicellulosiruptor bescii* exhibit enzyme stability and environmental adaptability. These two factors enable these organisms to perform optimally under extreme thermophilic temperatures [5,13,14]. Dark fermenters have an optimal pH range for hydrogen production of 5-7. On the other hand, photofermentative bacteria require a pH range of 6.8-7.5 for optimal performance [15,16]. The overall yields depend on factors like mass transfer efficiency and redox balance. These factors are affected by buffer composition, agitation rate, and gas sparging.

The optimized operating conditions are not the ultimate factors that can limit hydrogen production and output. The presence of heavy metals and the accumulation of end products, such as volatile fatty acids (VFAs) including acetate and butyrate, lead to pH drops that block hydrogen-evolving enzyme activity through enzymatic inhibition when their removal or recycling fails in the system [17,18]. The presence of other toxic substances from environmental pollutants and substrate breakdown products, including antibiotics, furfural, formaldehyde, nanoplastics, and lignocellulosic degradation products, can also disrupt cellular metabolic equilibrium and damage hydrogenase enzymes [19].

The production of high ammonia levels from a waste biomass rich in nitrogen, coupled with excessive substrate amounts, can drive fermentation toward acidogenic or solventogenic pathways. These pathways decrease hydrogen production while causing microbial damage [20,21]. The produced hydrogen is consumed by methanogenesis and other hydrogen-consuming processes carried out by methanogenic archaea and hydrogenotrophic bacteria. Maintaining high hydrogen production in batch and continuous bioreactors depends on strategies that block methanogenic activity, including the use of selective inhibitors, heat-treated inocula, and controlled operational settings [22,23].

Research on biohydrogen production urgently needs precise predictions, performance monitoring, and optimization of fermentation operations under specific environmental conditions. The biological systems that produce hydrogen through evolution exhibit complex, dynamic behavior. This is because microbial interactions, substrate conversion, and inhibitory feedback mechanisms create nonlinear responses [4,14]. The real-time operational dynamics of biohydrogen systems remain difficult to predict through linear models when operational parameters change. The modified Gompertz and modified Logistic models are among the most commonly used nonlinear kinetic models for analysis of biohydrogen systems [24]. These predictive models have enabled researchers to analyze hydrogen production curves and predict peak production rates and lag times. These predictions help them optimize their systems for scaling up and improving operational processes [25,26]. The analysis of nonlinear systems reveals detailed microbial reaction mechanisms and shows how systems respond to different inhibitors, pH levels, substrate concentrations, and temperature conditions. The process of model selection requires a comprehensive quantitative evaluation of the fitted data.

The use of direct visual or empirical fit methods for model evaluation can introduce several biases that may mask underlying predictive and mechanistic properties. As a result, the evaluation of models in recent times has included multiple standard error functions due to their importance such as the adjusted R-squared (adjR^2) serves as a measure of model fit, which adjusts for parameter count and penalizes models that overfit, Root Mean Square Error (RMSE) measures the typical difference between predicted and actual values of the response variable, which makes it a direct indicator of model performance, Mean Percentage Standard Deviation (MPSD) allows for the provision of a standardized error measurement. This step enables researchers to evaluate different datasets, and the Corrected Akaike Information Criterion (AICc) provides a balance between model fit and complexity, which proves essential for small sample sizes [26].

The evaluation of multiple error metrics, although it allows researchers to gain a complete understanding of model reliability and robustness, can become challenging when researchers base their choices on nonobjective or merely unanimous preferences or on visual assessments of models. To overcome these issues, the MOORA (Multi-Objective Optimization on the basis of Ratio Analysis) ranking system can provide an unbiased solution for model selection through multi-criteria decision analysis. The MOORA system for selecting primary models in biodegradation work, including biohydrogen production, has never been attempted, and Shukor was the first to use this approach in the biodegradation field to select the best model that governs degradation curves [27].

MOORA evaluates all selected error functions to generate an objective ranking of candidate models. This ranking eliminates the need for researcher-based decisions, which can be biased by preferences or human errors. The MOORA method enables researchers to evaluate models using normalized scores, producing systematic results for model comparison [28–30]. The combination of nonlinear models with multi-objective ranking systems for hydrogenogenic studies, as carried out in this study, is anticipated to accelerate laboratory-to-industry transitions while maintaining methodological sophistication that matches the biological intricacies of biohydrogen production systems.

MATERIALS AND METHODS

Fitting of the data

Using the Marquardt nonlinear regression approach, which minimizes the sum of squared residuals, biohydrogen production data from Figure 1 [31] were fitted to nonlinear equations (**Table 1**). This study utilized CurveExpert Professional software (Version 1.6). This iterative method achieves the best fit by minimizing the discrepancy between predicted and observed values. The program facilitates both manual and automated input of initial parameter estimates. A four-data point steepest ascent search yielded the maximum specific biohydrogen production rate (μ_m). The x-axis intercept of the projected line from the steepest ascent was utilized to determine the duration of the lag phase (λ). The final data point indicating the plateau period facilitated the estimation of the asymptotic value (A).

Table 1. Biohydrogen production models used in this study.

Model	*p*	Equation
Modified Logistic	3	$y = \frac{A}{1 + exp\left[\frac{4\mu_m}{A}(\lambda - t) + 2\right]}$
Modified Gompertz	3	$y = Aexp\left\{-exp\left[\frac{\mu_m . e}{A}(\lambda - t) + 1\right]\right\}$
Modified Richards	4	$y = A\left\{1 + vexp(1+v)exp\left[\frac{\mu_m}{A}(1+v)\left(1+\frac{1}{v}\right)(\lambda - t)\right]\right\}^{\left(\frac{-1}{v}\right)}$
Modified Schnute	4	$y = \left(\mu_m \frac{(1-\beta)}{\alpha}\right)\left[\frac{1-\beta exp(\alpha\lambda + 1 - \beta - \alpha t)}{1-\beta}\right]^{\frac{1}{\beta}}$
Baranyi-Roberts	4	$y = N_0 + \mu_m t + \frac{1}{\mu_m} ln(e^{-\mu_m t} + e^{-h_0} - e^{-\mu_m t - h_0}) - ln\left[1 + \frac{e^{\mu_m t + \frac{1}{\mu_m} ln(e^{-\mu_m t} + e^{-h_0} - e^{-\mu_m t - h_0})}}{e^{(A - N_0)}}\right]$
Von Bertalanffy	3	$y = k\left[1 - \left[1 - \left(\frac{A}{k}\right)^3\right] exp^{-\left(\frac{\mu_m t}{3k}\right)^{\frac{1}{3}}}\right]$
Huang	4	$y = A + \mu_m - ln\left(e^A + (e^{\mu_m} - e^A)e^{-\mu_m B(t)}\right)$ $B(t) = t + \frac{1}{\alpha} ln\frac{1 + e^{-\alpha(t-\lambda)}}{1 + e^{\alpha\lambda}}$
Buchanan Three-phase linear model	3	Y = N_0, IF X < LAG Y= N_0+ K(X−λ), IF λ ≤ X ≥ X_{MAX} Y = A, IF X ≥ X_{MAX}
Morgan-Mercer-Flodin (MMF)	4	$y = A - \frac{(A - \beta)}{1 + (\mu_m t)^{\delta}}$

Note:
A= Biohydrogen production upper asymptote;
N_0= Biohydrogen production lower asymptote;
u_m= maximum specific biohydrogen production rate;
v= affects near which asymptote maximum biohydrogen production occurs.
p = no of parameters
λ=lag time
e = exponent (2.718281828)
t = sampling time
α,β,*k*,δ = curve fitting parameters
h_0 = a dimensionless parameter quantifying the initial physiological state of the reduction process.
For the Baranyi-Roberts model, the lag time (λ) (h^{-1}) or (d^{-1}) can be calculated as h_0=μ_m
For modified Schnute, *A* =*m*/a

Statistical analysis

The following tests for statistical discrimination or error functions were used in this study, where n is the total number of observations, Obi and Pdi are the predicted and observed values, and p is the total number of model parameters [32].

RMSE was calculated using the following formula;

$$RMSE = \sqrt{\frac{\sum_{i=1}^{n}(Pd_i - Ob_i)^2}{n-p}} \quad \text{(Eqn. 1)}$$

BF and AF [33] were calculated using the following formula;

$$Bias\ factor = 10\left(\sum_{i=1}^{n} log\frac{(Pd_i/Ob_i)}{n}\right) \quad \text{(Eqn. 2)}$$

$$Accuracy\ factor = 10\left(\sum_{i=1}^{n} log\frac{|(Pd_i/Ob_i)|}{n}\right) \quad \text{(Eqn. 3)}$$

AICc [34,35] was calculated using the following formula;

$$AICc = 2p + n\ln\left(\frac{RSS}{n}\right) + \frac{2(p+1)+2(p+2)}{n-p-2} \quad \text{(Eqn. 4)}$$

BIC [36] was calculated using the following formula;

$$BIC = n\ln\left(\frac{RSS}{n}\right) + k\ln(n) \quad \text{(Eqn. 5)}$$

HQC [37] was calculated using the following formula;

$$HQC = nIn\left(\frac{RSS}{n}\right) + 2k\ln(\ln n) \quad \text{(Eqn. 6)}$$

Adjusted coefficient of determination (R^2) [38] was calculated using the following formula;

$$Adjusted\ (R^2) = 1 - \frac{RMS}{S_Y^2} \quad \text{(Eqn. 7)}$$

$$Adjusted\ (R^2) = 1 - \frac{(1-R^2)(n-1)}{(n-p-1)} \quad \text{(Eqn. 8)}$$

MPSD [39–41] was calculated using the following formula;

$$MPSD = 100\sqrt{\frac{1}{n-p}\sum_{i=1}^{n}\left(\frac{Ob_i - Pd_i}{Ob_i}\right)^2} \quad \text{(Eqn. 9)}$$

Application of Multi-Objective Optimization by Ratio Analysis (MOORA) in Modeling

The Multi-objective Optimization by Ratio Analysis (MOORA) was used for multi-criteria decision-making (MCDM) in the modeling exercise, as a combination of error-function superiority is frequently observed among the leading models. This method enables the identification of the best model by concurrently assessing various performance metrics. The methodology begins by normalizing the decision matrix to ensure comparability across performance metrics. The decision matrix was subsequently normalized. Due to the potential differences in units and magnitudes of these metrics, normalization must be performed using the following equation [27,29,42,43];

$$X'_{ij} = \frac{X_{ij}}{\sqrt{\sum_{i=1}^{n} X_{ij}^2}} \quad \text{(Eqn. 10)}$$

Where X_{ij} is the original value of the j^{th} metric for the i^{th} model, and X'_{ij} is the normalized value**.**

Ratio System Analysis

The normalized values were then aggregated using a ratio system approach. Beneficial criteria (those that should be maximized, $adjR^2$) were summed up, while non-beneficial criteria (the rest of the error functions) or those that should be minimized were subtracted using the following formula:

$$Y_i = \sum_{beneficial} X'_{ij} - \sum_{non-beneficial} X'_{ij} \quad \text{(Eqn. 11)}$$

Where Y_i is the final score for the i^{th} model

Weighted ratios should be used when certain criteria are more important. Weighted Ratios are not used because the literature has not agreed on which error functions are most important. Rating models by performance scores is the last step. High scores indicated excellence. Based on the decision criteria, the highest-valued model was best. This method objectively and systematically compared kinetic models to identify the best one, accounting for multiple performance metrics.

RESULTS AND DISCUSSION

The long-term operation of hydrogen-producing granular sludge in anaerobic reactors often results in the development of a complex microbial consortium with enhanced substrate conversion efficiency. Such consortia possess diverse metabolic capabilities for sucrose fermentation and hydrogen generation, making biological dark fermentation an ideal approach for sustainable biohydrogen production. Despite extensive experimental research, only a limited number of primary kinetic models have been applied to describe the growth behavior and hydrogen production dynamics of these systems. In this study, the growth data for H_2-producing granular sludge obtained from a packed-bed upflow reactor operated at 26 °C on sucrose-containing wastewater for over 500 days were first transformed to the natural logarithm (**Fig. 1**) prior to modeling using several predictive growth equations.

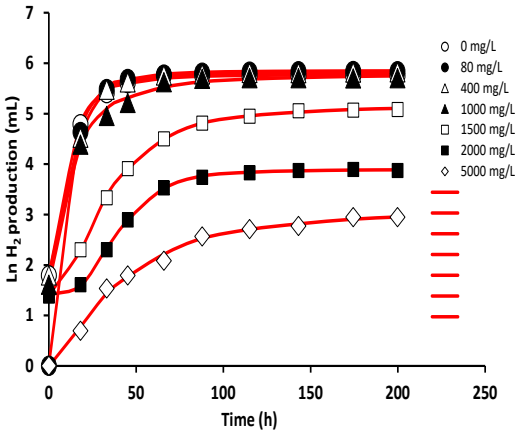

Fig. 1. Modelling the growth kinetics of H_2-producing granular sludge sampled from a packed-bed upflow reactor (operated at 26 °C treating sucrose-containing wastewater for >500 days) using the x model at various Zn concentrations.

Bacterial biohydrogen production often exhibits a sigmoidal profile similar to bacterial growth, with a distinct adaptation phase in which the specific growth rate is near zero and gradually increases to the maximal value (μ_{max}). This results in an observable lag time (λ) [44]. In the sigmoidal growth pattern, the lag period indicates a period of cellular adjustment during which hydrogen-producing bacteria acclimate to new environmental or substrate conditions. This adjustment is particularly important following inoculum storage or adaptation to fresh media. The lag phase is where cells synthesize key enzymes and cofactors. These compounds are required for hydrogenogenic metabolism to support exponential growth [45]. Baranyi and Roberts [46] suggested that this preparatory period represents a transitional phase that bridges two autonomous growth systems.

The incorporation of lag time or related parameters into kinetic models is mainly a pragmatic choice to describe growth dynamics rather than to provide a mechanistic explanation. The most important estimated parameters—especially the maximum specific growth rate (μ_m)—can then be used for secondary predictive modeling and optimization of hydrogen yield. The effect of the substrate on the growth rate can be modeled using the secondary models of Monod, Haldane, Aiba, and Teissier. These models are often applied to explain the inhibitory effects of substrate, especially at high concentrations, and the potential inhibition of bacterial growth by heavy metals on hydrogen evolution rates. These models allow us to understand how varying substrate levels and environmental stresses influence the metabolism of microorganisms (metavolism), a feature that will be important for optimizing biohydrogen production systems, improving process stability, and enhancing the overall energy conversion efficiency [47,48]. Various primary models (**Figs. 2-10)** were used to fit the hydrogen production rate, and most of them show visually acceptable fits. The best model, based on statistical analysis, was the MMF model, with the highest value for the adjusted coefficient of determination and the lowest values for RMSE, BIC, HQC, and AICc, and the accuracy and bias factors were in the optimal range (**Table 2**). **Table 2** presents the ranking of nine kinetic models based on their MOORA (Multi-Objective Optimization by Ratio Analysis) scores for fitting hydrogen production over time. The Morgan–Mercer–Flodin (MMF) model achieved the highest MOORA score (2.09020). This is followed by the Modified Logistic (ML) and Modified Schnute (MS) models, which indicate a superior overall performance across multiple error-based criteria.

Models such as modified Gompertz (MG), Huang (HG), and von Bertalanffy (VB) displayed moderate suitability, while Buchanan-3 -phase (B3P), Baranyi-Roberts (BR), and particularly modified Richards (MR) performed poorly, which yields a negative MOORA score (–0.03732), indicating its weak predictive capability. The MOORA method allows effective discrimination between models even when the combinations of error metrics were not unanimous. In the original publication, only the modified Gompertz model was utilized [31]. MOORA integrates multiple evaluation parameters (e.g., RMSE, R^2, SSE) into a single composite score. This multi-criteria approach is MOORA's central strength, enabling it to identify the most accurate and stable predictive models and provide a clear hierarchical ranking among models with otherwise conflicting performance indicators. Modelling results using the MMF models at various concentrations of zinc. The cumulative hydrogen production profiles of sucrose-fed granular sludge under different zinc (Zn) concentrations are shown in **Fig. 11**.

The experimental data follow the Morgan–Mercer–Flodin (MMF) model accurately. The hydrogen production rates increased steeply during the initial phase, then decreased until a stable production level was achieved. Fast production rates at low Zn concentrations (0-400 mg/L) occurred because zinc supports essential microbial metabolic processes and enzymatic activities, especially hydrogenogenesis. A decrease in the total hydrogen production occurred at elevated Zn concentrations of 1000–1500 mg/L and especially so between 2000 and 5000 mg/L where a near complete hydrogen production occurs likely due to toxic levels restricted microbial growth and substrate conversion efficiency (**Fig. 11**). The MMF model successfully modeled all the phases of the sigmoidal cumulative hydrogen production data at all tested Zn concentrations (**Fig. 12**). To reiterate, the specific hydrogen production rate reached its maximum value of 0.08 h^{-1} as zinc acts as a micronutrient that boosted microbial enzymatic activity at low level including hydrogenase ctivity. At high Zn concentrations, a severe metabolic suppression occurred.

In predictive modelling of microbial processes, converting growth or hydrogen production data to the natural logarithm (ln) form is necessary for accurate kinetic modelling. Biological systems often exhibit nonlinear behavior, and taking the ln allows linearization of this phase, which simplifies the estimation of the rate constants and improvess model fitting using nonlinear models such as the Morgan–Mercer–Flodin or the modified Gompertz models. This linearizing transformation also allows for the stabilization of the variance. This standardization ensures a constant error distribution and meets the assumptions of regression. By converting multiplicative biological effects to a

linear form, this enhances the interpretability of the parameters, including the specific production rate and lag period. In hydrogen production studies, ln-transformed data can better capture the transition from the exponential to the stationary phase, enabling smoother predictive modeling. Overall, the ln transformation can improve statistical reliability, reduce heteroscedasticity, and provide better biological insights. Thus, linearization allows a standard preprocessing step for analyzing predictive bioprocess models, including biohydrogen production [49–52].

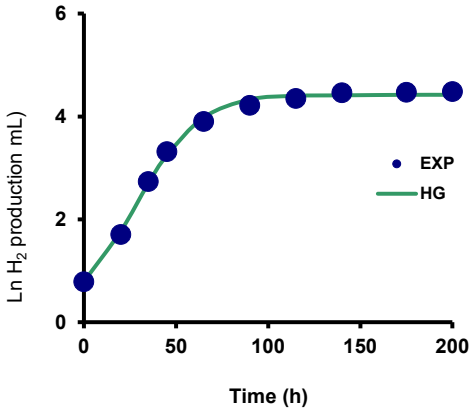

Fig. 2. Modelling the growth kinetics of H_2-producing granular sludge sampled from a packed-bed upflow reactor (operated at 26 °C treating sucrose-containing wastewater for >500 days) using the Huang model.

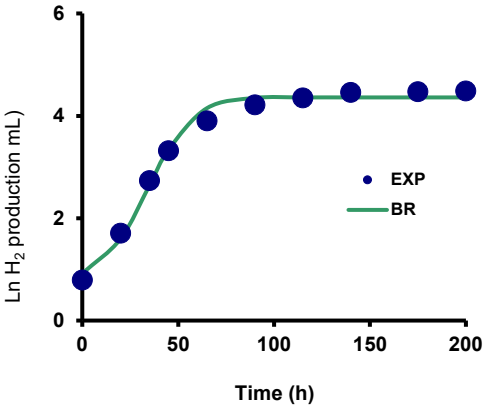

Fig. 3. Modelling the growth kinetics of H_2-producing granular sludge from the packed-bed upflow reactor using the Baranyi–Roberts model.

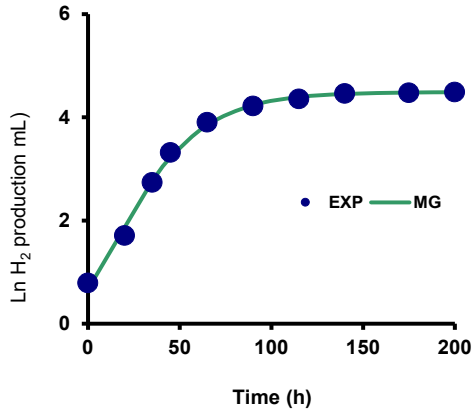

Fig. 4. Predictive modelling of cumulative hydrogen-producing activity of granular sludge (26 °C, sucrose-fed reactor) using the Modified Gompertz model.

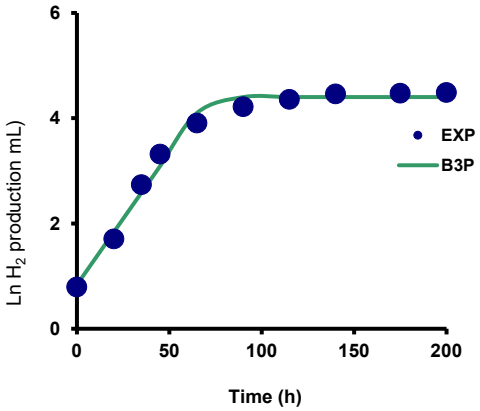

Fig. 5. Growth curve simulation of H_2-producing granular sludge from long-term sucrose-fed reactor operation fitted to the Buchanan three-phase model.

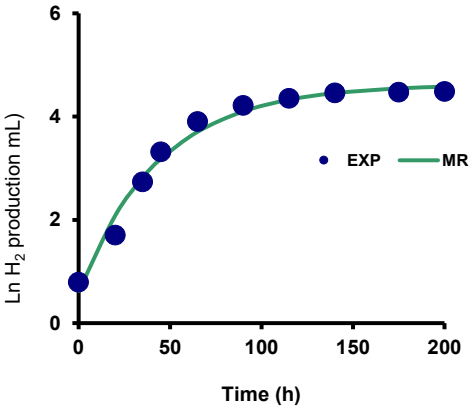

Fig. 6. Fitting experimental hydrogenogenic growth data of granular sludge from the packed-bed reactor to the Modified Richards model.

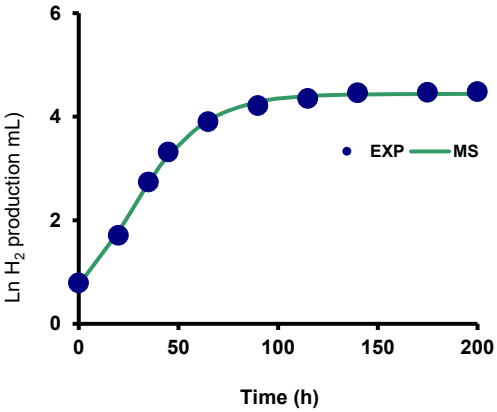

Fig. 7. Evaluation of hydrogen production growth profile of granular sludge using the Modified Schnute model under mesophilic sucrose fermentation conditions.

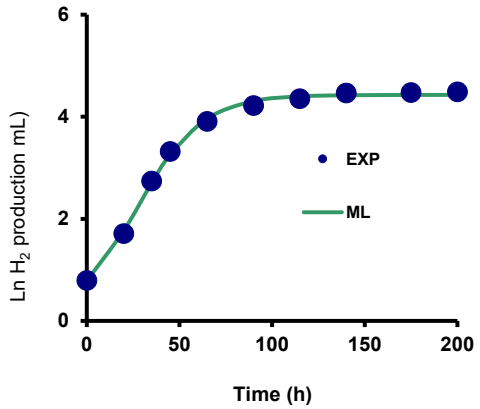

Fig. 8. Simulation of microbial growth kinetics of H_2-producing granular sludge (from 26 °C reactor) using the Modified Logistic model.

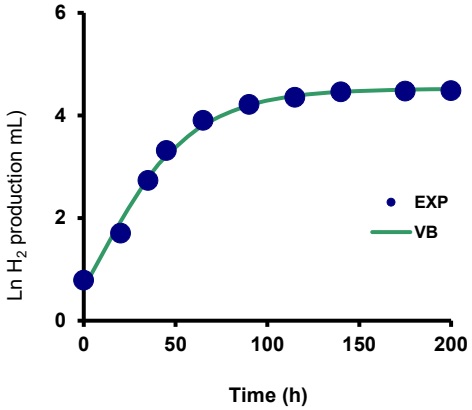

Fig. 9. Modelling the hydrogenogenic biomass development of granular sludge sampled from the upflow reactor using the von Bertalanffy model.

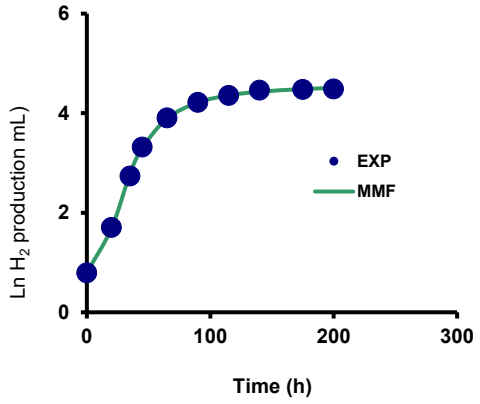

Fig. 10. Predictive fitting of cumulative hydrogen production data of granular sludge (sucrose wastewater-fed reactor) using the Morgan–Mercer–Flodin (MMF) model.

Table 2. Statistical analysis of the growth models.

Model	P	MPSD	RMSE	R^2	adR^2	AICc	BIC	HQC	BF	AF
HG	4	8.34	0.083	1.00	0.995	-21.797	-45.59	-48.12	1.002	1.010
BR	4	16.08	0.161	0.99	0.982	-8.662	-32.45	-34.99	1.002	1.017
MG	3	8.87	0.089	1.00	0.995	-30.011	-45.10	-47.01	1.000	1.003
B3P	3	16.19	0.162	0.99	0.982	-17.982	-33.07	-34.98	1.005	1.015
MR	4	20.95	0.210	0.98	0.97	-3.365	-27.15	-29.69	0.995	1.012
MS	4	6.77	0.068	1.00	0.997	-25.976	-49.77	-52.30	1.001	1.006
ML	3	6.67	0.067	1.00	0.997	-35.725	-50.82	-52.72	1.002	1.008
VB	3	11.78	0.118	0.99	0.991	-24.334	-39.43	-41.33	0.999	1.005
MMF	4	2.69	0.027	1.00	0.999	-44.399	-68.19	-70.73	1.000	1.002

Note:
p parameter
RMSE Root Mean Square Error
R^2 Coefficient of Determination
adR^2 Adjusted Coefficient of Determination
AICC Corrected Akaike Information Criterion
BF Bias Factor
AF Accuracy Factor
n.a. Not available

Table 3. Model ranking using MOORA method to effectively distinguishes predictive accuracy among the models.

No	Model	MOORA Score	Rank
1	MMF	2.09020	1
2	ML	1.50559	2
3	MS	1.36732	3
4	MG	1.23058	4
5	HG	1.16664	5
6	VB	0.91489	6
7	B3P	0.49653	7
8	BR	0.37934	8
9	MR	-0.03732	9

The original intent in developing the MMF model was to provide a model that can relate the wide variety of nutrient-response relationships observed in animals [53]. The growth of animals such as sheep, rabbits, and horses, as well as that of microorganisms, can now be successfully modeled [54–60]. The MMF model has also been used to model exopolysaccharide production by *Klebsiella oxytoca* [61], yeast growth [62], oil palm yield over time [63], ethanol production [64], and even total human deaths caused by COVID-19 complications [65–70]. One of the most recent uses of the model is in the modelling of the inhibitory effect of Zn on the biodegradation of SDS [71]. Similar to the modified Gompertz model, the MMF model even has uses in modelling financial growth [72].

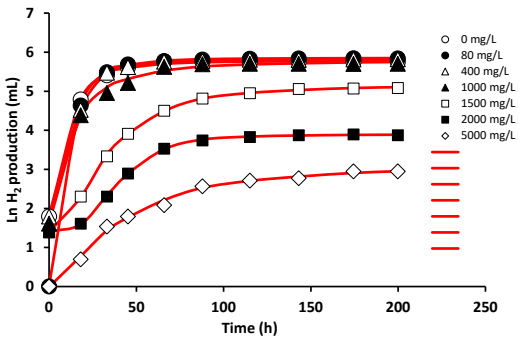

Fig. 11. Fitting (red lines) of cumulative hydrogen production data of granular sludge (sucrose wastewater-fed reactor) at various Zn concentrations using the Morgan–Mercer–Flodin (MMF) model.

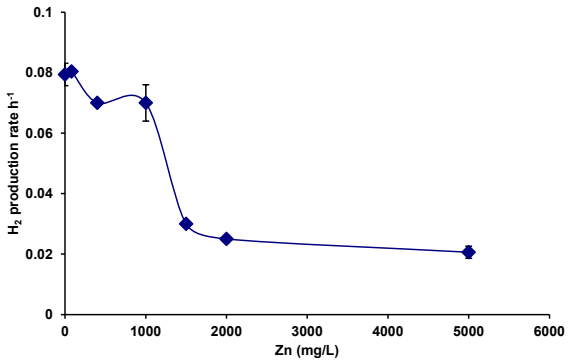

Fig. 12. Effect of zinc (Zn) concentration on the specific biohydrogen production rate by sucrose-fed granular sludge. The experimental data were fitted using the Morgan–Mercer–Flodin (MMF) model.

In microbial kinetics, accurately modeling bacterial growth and the inhibitory effects of substrates is essential for optimizing bioprocesses, ensuring product safety, and understanding microbial ecology.

Primary models such as the modified Gompertz, modified Logistic, modified Richards, Baranyi-Roberts, modified Schnute, von Bertalanffy, and Morgan-Mercer-Flodin (MMF) and Huang models are pivotal in this endeavor. These models describe bacterial growth under non-inhibitory conditions and estimate vital parameters, including specific growth rate (μ_m), lag phase duration, and maximum population density. Understanding these parameters is crucial for advancing to more complex secondary modeling that incorporates inhibitory effects using models such as the Haldane, Andrews, Yano, and Aiba models.

These primary models are instrumental in determining key growth parameters — fundamental to microbiology and biochemical engineering — and in defining the replication speed of bacteria under specific conditions. By providing detailed insights into bacterial growth dynamics, these models enable researchers to predict how bacteria will respond to various environmental changes and nutrient availability, which is vital for applications such as wastewater treatment, bioremediation, and the production of biofuels and other bioproducts [44,73–76].

Table 4. Summary of the optimization of biohydrogen production by various microorganisms.

Microorganism / Consortium	Optimum Conditions	Maximum Biohydrogen Production	Main Inhibitory Factors	Inhibitory Model Used	Predictive Model Used	References
Clostridium butyricum / *Clostridium* spp.	pH 5.5–7.0, 30–37 °C, anaerobic	2–3 mol H_2/mol glucose	VFAs, heavy metals, substrate overload	Modified Andrews, Han-Levenspiel (metal and substrate inhibition)	Modified Gompertz, Logistic, Luedeking–Piret	[11,31,77]
Clostridium pasteurianum	pH 6.0–6.8, 35 °C	2.8 mol H_2/mol glucose	Phenol, cresol, furfural	Modified Han-Levenspiel (inhibitor toxicity)	Modified Gompertz	[83,84]
Thermotoga neapolitana / *maritima*	pH 6–7, 65–80 °C, extreme thermophile	3–4.5 mol H_2/mol glucose	Ammonia, acetate accumulation	No inhibitory model applied	Modified Gompertz, First-order, Luedeking–Piret	[25,85]
Caldicellulosiruptor bescii	pH 6–7, 70–75 °C	1.8–2.2 mol H_2/mol glucose eq.	Phenolic compounds, NH_3	None (empirical inhibition)	Modified Gompertz	[5]
Enterobacter cloacae / *aerogenes*	pH 6–7, 30–40 °C	~2 mol H_2/mol glucose	Antibiotics, substrate overload	Modified Han-Levenspiel (Cu, Fe inhibition)	Modified Gompertz, Logistic, First-order	[6,79]
Ethanoligenens harbinense B49	pH 5.5–6.7, 35–40 °C	2.4 mol H_2/mol hexose	Acetate, ethanol	None reported	Modified Gompertz	[18]
Thermoanaerobacterium thermosaccharolyticum	pH 6–7, 55–65 °C	2.5 mol H_2/mol glucose	High ammonia, VFA	Modified Han-Levenspiel (product inhibition)	Modified Gompertz, Monod-type	[78,78]
Caloramator celer	pH 7–8, 65 °C	~1.9 mol H_2/mol glucose	Substrate inhibition	Modified Andrews	Modified Gompertz, Logistic	[86]
Mixed anaerobic consortia (sludge-based)	pH 5–7, 30–70 °C	0.5–2 L H_2/L·d	VFAs, NH_3, nanoplastics	Modified Han-Levenspiel (acetate inhibition)	Modified Gompertz, First-order, Monod	[9,19,87]
Rhodobacter sphaeroides (photofermentative)	pH 6.8–7.3, 28–35 °C, light	1.5–4 mol H_2/mol acetate/lactate	NH_4^+, light limitation	None	Modified Gompertz, Logistic	[82,88]
Rhodopseudomonas palustris	pH 6–8, 30–35 °C, light	Up to 7 mol H_2/mol substrate	Excess substrate, byproducts	None	Modified Gompertz, Luedeking–Piret, Monod	[81,89]
Rhodobacter capsulatus	pH 7.0, 30 °C	3–4 mol H_2/mol acetate	Ammonium regulation	None	Modified Gompertz	[90]
Microalgae (e.g., *Chlamydomonas reinhardtii*)	pH 7–8, 20–30 °C, light	11 mL H_2/L·h	O_2, heavy metals	None	Modified Gompertz, Light-response logistic	[10]
Azotobacter vinelandii	Aerobic, 28–32 °C	Up to 1.5 mmol H_2/L·h	Nitrogenous compounds	None	Luedeking–Piret	[91]
Klebsiella oxytoca GS-4-08	pH 6–7, 30–35 °C	2.8 mol H_2/mol xylose	Substrate inhibition	Haldane/Modified Andrews	Modified Gompertz, Monod	[80]
Thermoanaerobacter GHL15	pH 6.5–7, 70 °C	3.5 mol H_2/mol glucose	Substrate inhibition	Modified Andrews	Modified Gompertz	[13]
Citrobacter sp. Y19	pH 6.8–7.0, 37 °C	2.9 mol H_2/mol glucose	O_2 presence	None	Modified Gompertz	[92]
Bacillus sp. / Biofilm consortia	pH 6–7, 37–45 °C	1.8–2.2 mol H_2/mol substrate	VFAs, heavy metals	Modified Han-Levenspiel, Andrews	Modified Gompertz, First-order	[7,93]

The MMF model is rarely used to model biohydrogen production. Most often, the modified Gompertz model is a widely applied kinetic tool in biohydrogen research, providing a simple yet physiologically meaningful framework for estimating maximum hydrogen potential (H_{max}), production rate (R_{max}), and lag time (λ). It effectively captures sigmoidal hydrogen production in *Clostridium* systems, describing adaptation, exponential, and saturation phases under varying substrate and metal conditions [11,31]. Integrating Gompertz kinetics with Luedeking–Piret equations improves scale-up predictability [77]. The model remains valid for thermophiles such as *Thermotoga neapolitana* and *Caldicellulosiruptor bescii*, achieving $R^2 > 0.97$ at 80 °C [25,78].

For facultative anaerobes like *Enterobacter cloacae* and *Klebsiella oxytoca*, it accurately predicts hydrogen yield under substrate or inhibitor stress [6,79,80]. Photofermenters such as *Rhodobacter sphaeroides* and microalgae *Chlamydomonas reinhardtii* also fit the model under variable light regimes [10,81,82]. Overall, the Modified Gompertz model remains the most popular for linking microbial hydrogen kinetics with process optimization and scale-up design (Table 4), and in most cases these reports use only the MG model despite the availability of other, more suitable models, including MMF. The reason for this is likely a lack of knowledge and awareness of the presence of other predictive models.

CONCLUSION

This study demonstrated that the Morgan–Mercer–Flodin (MMF) model provides excellent predictive capabilities for understanding hydrogen production kinetics in granular sludge systems. The MMF model outperformed traditional primary models, including the Modified Gompertz, by providing precise simulations of complete hydrogen production phases and correctly representing zinc's dual effects on the process. The application of logarithmic data transformation techniques resulted in more stable model performance, which led to reliable parameter estimation. The MOORA-based evaluation system used multiple criteria to select the most precise and dependable kinetic predictive models for ranking. This study demonstrates that the Modified Gompertz model should not be the default choice for biohydrogen studies, as other predictive models, such as the MMF model, offer greater flexibility and a more detailed mechanistic understanding. The research results enable better optimization of biohydrogen reactor operating conditions, leading to improved process stability and the development of essential modeling tools for large-scale sustainable hydrogen production.

REFERENCES

1. Elbeshbishy E, Dhar BR, Nakhla GF, Lee HS. A critical review on inhibition of dark biohydrogen fermentation. Renew Sustain Energy Rev. 2017;79:656–68.
2. Zheng H, Zeng RJ, Angelidaki I. Biohydrogen production from glucose in upflow biofilm reactors with plastic carriers under extreme thermophilic conditions (700C). Biotechnol Bioeng. 2008;100(5):1034–8.
3. Levin DB, Carere RC, Çiçek N, Sparling RR. Challenges for biohydrogen production via direct lignocellulose fermentation. Int J Hydrog Energy. 2009;34(17):7390–403.
4. Bielen AAM, Verhaart MRA, van der Oost J, Kengen SWM. Biohydrogen production by the thermophilic bacterium Caldicellulosiruptor saccharolyticus: Current status and perspectives. Life. 2013;3(1):52–85.
5. Tunca B, Kutlar FE, Kas A, Yilmazel YD. Enhanced biohydrogen production from high loads of unpretreated cattle manure by cellulolytic bacterium Caldicellulosiruptor bescii at 75 °C. Waste Manag. 2023;171:401–10.
6. Pachapur VL, Sarma SJ, Brar SK, Le Bihan Y, Buelna G, Verma M. Biohydrogen production by co-fermentation of crude glycerol and apple pomace hydrolysate using co-culture of Enterobacter aerogenes and clostridium butyricum. Bioresour Technol. 2015;193:297–306.
7. Goud RK, Raghavulu SV, Mohanakrishna G, Naresh K, S. VM. Predominance of Bacilli and Clostridia in microbial community of biohydrogen producing biofilm sustained under diverse acidogenic operating conditions. Int J Hydrog Energy. 2012;37(5):4068–76.
8. García-Depraect O, Rene ER, Diaz-Cruces VF, León-Becerril E. Effect of process parameters on enhanced biohydrogen production from tequila vinasse via the lactate-acetate pathway. Bioresour Technol. 2019;273:618–26.
9. Sarkar O, Rova U, Christakopoulos PF, Matsakas L. Continuous biohydrogen and volatile fatty acids production from cheese whey in a tubular biofilm reactor: Substrate flow rate variations and microbial dynamics. Int J Hydrog Energy. 2024;59:1305–16.
10. El-Dalatony MM, Zheng Y, Ji M, Li X, Salama ES. Metabolic pathways for microalgal biohydrogen production: Current progress and future prospectives. Bioresour Technol. 2020;318.
11. Monlau F, Aemig Q, Trably E, Hamelin J, Steyer JP, Carrère H. Specific inhibition of biohydrogen-producing Clostridium sp. after dilute-acid pretreatment of sunflower stalks. Int J Hydrog Energy. 2013;38(28):12273–82.
12. Rai P, Pandey AC, Pandey A. Optimization of sugar release from banana peel powder waste (BPPW) using box-behnken design (BBD): BPPW to biohydrogen conversion. Int J Hydrog Energy. 2019;44(47):25505–13.
13. Brynjarsdóttir H, Scully SM, Örlygsson J. Production of biohydrogen from sugars and lignocellulosic biomass using Thermoanaerobacter GHL15. Int J Hydrog Energy. 2013;38(34):14467–75.
14. Zheng G, Kang Z, Qian Y, Wang L, Zhou Q, Zhu H. Biohydrogen production from tofu wastewater with glutamine auxotrophic mutant of Rhodobacter sphaeroides. In: AIP Conference Proceedings. 2008. p. 143–8.
15. García AB, Cammarota MC. Biohydrogen production from pretreated sludge and synthetic and real biodiesel wastewater by dark fermentation. Int J Energy Res. 2019;43(4):1586–96.
16. Park J hoon, Yoon JJ, Park H, Kim Y, Lim D jung, Kim SH. Feasibility of biohydrogen production from Gelidium amansii. Int J Hydrog Energy. 2011;36(21):13997–4003.
17. van Ginkel SW, Logan BE. Inhibition of biohydrogen production by undissociated acetic and butyric acids. Environ Sci Technol. 2005;39(23):9351–6.
18. Tang J, Yuan Y, Guo W, Ren N. Inhibitory effects of acetate and ethanol on biohydrogen production of Ethanoligenens harbinese B49. Int J Hydrog Energy. 2012;37(1):741–7.
19. Alam M, Mostafa A, Dhar BR. Impact of petroleum versus bio-based nano/microplastics on fermentative biohydrogen production from sludge. Int J Hydrog Energy. 2024;94:959–70.
20. Tratzi P, Ta DT, Zhang Z, Torre M, Battistelli F, Manzo E, et al. Sustainable additives for the regulation of NH3 concentration and emissions during the production of biomethane and biohydrogen: A review. Bioresour Technol. 2022;346.
21. Salerno MB, Park W, Zuo Y, Logan BE. Inhibition of biohydrogen production by ammonia. Water Res. 2006;40(6):1167–72.
22. Chae KJ, Choi M, Kim KY, Ajayi FF, Chang IS, Kim IS. Selective inhibition of methanogens for the improvement of biohydrogen production in microbial electrolysis cells. Int J Hydrog Energy. 2010;35(24):13379–86.
23. Hafez H, Elbeshbishy E, Nakhla GF, El Naggar HM. Simulating the impact of suppression of methanogenesis in continuous flow biohydrogen reactors. Int J Hydrog Energy. 2011;36(10):5885–94.
24. Nemestóthy N, Bakonyi P, Rózsenberszki T, Kumar G, Koók L, Kelemen G, et al. Assessment via the modified gompertz-model reveals new insights concerning the effects of ionic liquids on biohydrogen production. Int J Hydrog Energy. 2018;43(41):18918–24.
25. Frascari D, Cappelletti M, Mendes JDS, Alberini A, Scimonelli F, Manfreda C, et al. A kinetic study of biohydrogen production from glucose, molasses and cheese whey by suspended and attached cells of Thermotoga neapolitana. Bioresour Technol. 2013;147:553–61.

26. Mohanty K, Das D. Kinetics of biohydrogen production by dark fermentation processes. 2012;127–36.
27. Halmi MIE, Syed MA, Shamaan NA, Shukor MY. Mathematical Modeling of Molybdenum Reduction to Molybdenum Blue by Burkholderia sp. Strain Dr.Y27 and Model Selection Using the MOORA Method. J Environ Bioremediation Toxicol. 2024 Dec 26;7(2):17–24.
28. Barik T, Parida S, Pal K. Optimizing Process Parameters in Drilling of CFRP Laminates: A Combined MOORA–TOPSIS–VIKOR Approach. Fibers Polym. 2024 May 1;25(5):1859–76.
29. Brauers W. Multi-objective seaport planning by MOORA decision making. Ann Oper Res. 2013 July 1;206.
30. Brauers WKM, Zavadskas EK, Peldschus F, Turskis Z. Multi-objective decision-making for road design. Transport. 2008 Jan 1;23(3):183–93.
31. Li C, Fang HHP. Inhibition of heavy metals on fermentative hydrogen production by granular sludge. Chemosphere. 2007 Mar;67(4):668–73.
32. Motulsky HJ, Ransnas LA. Fitting curves to data using nonlinear regression: a practical and nonmathematical review. FASEB J. 1987;1(5):365–74.
33. Ross T. Indices for performance evaluation of predictive models in food microbiology. J Appl Bacteriol. 1996;81(5):501–8.
34. Akaike H. A New Look at the Statistical Model Identification. IEEE Trans Autom Control. 1974;19(6):716–23.
35. Burnham KP, Anderson DR. Multimodel inference: Understanding AIC and BIC in model selection. Sociol Methods Res. 2004;33(2):261–304.
36. Schwarz G. Estimating the Dimension of a Model. Ann Stat. 1978;6(2):461–4.
37. Hannan EJ, Quinn BG. The Determination of the Order of an Autoregression. J R Stat Soc Ser B Methodol. 1979;41(2):190–5.
38. Ezekiel M. The Sampling Variability of Linear and Curvilinear Regressions: A First Approximation to the Reliability of the Results Secured by the Graphic 'Successive Approximation' Method. Ann Math Stat. 1930;1(4):275–333.
39. Marquardt DW. An Algorithm for Least-Squares Estimation of Nonlinear Parameters. J Soc Ind Appl Math. 1963;11(2):431–41.
40. Seidel A, Gelbin D. On applying the ideal adsorbed solution theory to multicomponent adsorption equilibria of dissolved organic components on activated carbon. Chem Eng Sci. 1988 Jan 1;43(1):79–88.
41. Porter JF, McKay G, Choy KH. The prediction of sorption from a binary mixture of acidic dyes using single- and mixed-isotherm variants of the ideal adsorbed solute theory. Chem Eng Sci. 1999;54(24):5863–85.
42. Karel W, Brauers W, Zavadskas E. The MOORA method and its application to privatization in a transition economy. Control Cybern. 2006 Jan 1;35.
43. Shukor MY. Chitosan–Silica Composite Aerogel for the Adsorption of Cupric Ions: Isothermal Remodeling and MOORA-Based Model Selection. J Environ Microbiol Toxicol. 2024 Dec 26;12(2):53–62.
44. McClure PJ, Cole MB, Davies KW. An example of the stages in the development of a predictive mathematical model for microbial growth: the effects of NaCl, pH and temperature on the growth of Aeromonas hydrophila. Int J Food Microbiol. 1994;23(3–4):359–75.
45. Karthic P, Joseph S, Arun N, Varghese LA, Santhiagu A. Biohydrogen production using anaerobic mixed bacteria: Process parameters optimization studies. J Renew Sustain Energy. 2013;5(6).
46. Baranyi J, Roberts TA. A dynamic approach to predicting bacterial growth in food. Int J Food Microbiol. 1994;23(3–4):277–94.
47. Agarry SE, Audu TOK, Solomon BO. Substrate inhibition kinetics of phenol degradation by *Pseudomonas fluorescence* from steady state and wash-out data. Int J Environ Sci Technol. 2009;6(3):443–50.
48. Othman AR, Bakar NA, Halmi MIE, Johari WLW, Ahmad SA, Jirangon H, et al. Kinetics of molybdenum reduction to molybdenum blue by *Bacillus* sp. strain A.rzi. BioMed Res Int. 2013;2013:Article number 371058.
49. Abubakar A, Uba G, Biu HA. Kinetics Modelling of Pseudomonas stutzeri strain DN2 Growth Behaviour in Tributyltin Chloride. J Environ Microbiol Toxicol. 2021 Dec 31;9(2):13–8.
50. Arroyo-López FN, Bautista-Gallego J, Durán-Quintana MC, Garrido-Fernández A. Modelling the inhibition of sorbic and benzoic acids on a native yeast cocktail from table olives. Food Microbiol. 2008 June 1;25(4):566–74.
51. Baty F, Delignette-Muller ML. Estimating the bacterial lag time: Which model, which precision? Int J Food Microbiol. 2004;91(3):261–77.
52. Buchanan RL. Developing and distributing user-friendly application software. J Ind Microbiol. 1993;12(3–5):251–5.
53. Morgan PH, Mercer LP, Flodin NW. General model for nutritional responses of higher organisms. Proc Natl Acad Sci. 1975 Nov 1;72(11):4327–31.
54. Santos SA, Souza G da S e, Oliveira MR de, Sereno JR. Uso de modelos não-lineares para o ajuste de curvas de crescimento de cavalos pantaneiros. Pesqui Agropecuária Bras. 1999 July;34(7):1133–8.
55. Topal M, Bolukbasi ŞC. Comparison of nonlinear growth curve models in broiler chickens. J Appl Anim Res. 2008 Dec 1;34(2):149–52.
56. Tariq M, Iqbal F, Eyduran E, Bajwa M, Huma Z, Waheed A. Comparison of nonlinear functions to describe the growth in Mengali sheep breed of Balochistan. Pak J Zool. 2013 June 1;45:661–5.
57. Augustine A, Imelda J, Paulraj R, David NS. Growth kinetic profiles of *Aspergillus niger* S14 a mangrove isolate and *Aspergillus oryzae* NCIM 1212 in solid state fermentation. Indian J Fish. 2015;62(3):100–6.
58. Kemper CM. Growth and development of the brush-tailed rabbit-rat (*Conilurus penicillatus*), a threatened tree-rat from northern Australia. Aust Mammal. 2020 June 5;
59. Yahuza S, Sabo IA. Mathematical Modelling of the Growth of *Bacillus cereus* Strain wwcp1on Malachite Green Dye. J Biochem Microbiol Biotechnol. 2021 Dec 31;9(2):25–9.
60. Giacon TG, de Gois e Cunha GC, Eliodório KP, Oliveira RP de S, Basso TO. Homo- and heterofermentative lactobacilli are distinctly affected by furanic compounds. Biotechnol Lett. 2022 Dec 1;44(12):1431–45.
61. Tomulescu C, Moscovici M, Stoica R, Albu G, Sevcenco C, Vamanu A. Investigation of culture conditions by Response Surface Methodology and kinetic modeling for exopolysaccharide production by Klebsiella oxytoca ICCF 419 strain, using lactose as substrate. Romanian Biotechnol Lett. 2020 Aug 18;25:2033–44.
62. Carvalho ÂR, Genz Bazana LC, Ferrão MF, Fuentefria AM. Curve fitting and linearization of UV–Vis spectrophotometric measurements to estimate yeast in inoculum preparation. Anal Biochem. 2021 July 15;625:114216.
63. Khamis A, Ismail Z, Haron K, Mohammed AT. Nonlinear Growth Models for Modeling Oil Palm Yield Growth. J Math Stat. 2005 Sept 30;1(3):225–33.
64. Germec M, Turhan I. Ethanol production from acid-pretreated and detoxified tea processing waste and its modeling. Fuel. 2018 Nov 1;231:101–9.
65. Aisami A, Shukor MYA. Predictive Mathematical Modelling of the Total Number of COVID-19 Cases for the Kingdom of Saudi Arabia. J Environ Microbiol Toxicol. 2020 July 31;8(1):11–5.
66. Yahuza S, Sabo IA, Dan-Iya BI, Shukor MYY. Prediction of Cumulative Death Cases in Nigeria Due to COVID-19 Using Mathematical Models. Bull Environ Sci Sustain Manag. 2020 July 31;4(1):20–4.
67. Shukor MYA, Sabo IA, Yahuza S, Dan-Iya BI, Wada SA. Prediction of Cumulative Death Cases in The United States Due to COVID-19 Using Mathematical Models. J Environ Microbiol Toxicol. 2020 July 31;8(1):37–41.
68. Uba G, Yakasai HM, Abubakar A, Shukor MYY. Prediction of Cumulative Death Cases in Brazil Due to Covid-19 Using Mathematical Models. Bull Environ Sci Sustain Manag. 2020 July 31;4(1):13–9.
69. Yakasai HM, Shukor MYA. Predictive Mathematical Modelling of the Total Number of COVID-19 Cases for The United States. Bioremediation Sci Technol Res. 2020 July 31;8(1):11–6.
70. Aisami AB, Umar AM, Shukor MYA. Prediction of Cumulative Death Cases in Indonesia Due to COVID-19 Using Mathematical Models. Bioremediation Sci Technol Res. 2020 July 31;8(1):32–6.
71. Rusnam, Syafrawati S, Khayat ME, Nasution FI, Yakasai HM, Abubakar A. Primary Mathematical Modeling of the Growth of

SDS by a bacterium Isolated From a Paddy Field. J Environ Microbiol Toxicol. 2024 July 31;12(1):23–30.
72. Wijeratne AW, Karunaratne JA. Morgan-Mercer-Flodin model for long term trend analysis of currency exchange rates of some selected countries. Int J Bus Excell. 2013 Dec 2;7(1):76–87.
73. Manogaran M, Othman AR, Shukor MY, Halmi MIE. Modelling the Effect of Heavy Metal on the Growth Rate of an SDS-degrading *Pseudomonas* sp. strain DRY15 from Antarctic soil. Bioremediation Sci Technol Res. 2019 July 31;7(1):41–5.
74. Shukor MS, Shukor MY. Bioremoval of toxic molybdenum using dialysis tubing. Chem Eng Res Bull. 2015;18(1):6–11.
75. Sevinç P, Gündüz U, Eroglu I, Yücel M. Kinetic analysis of photosynthetic growth, hydrogen production and dual substrate utilization by *Rhodobacter capsulatus*. Int J Hydrog Energy. 2012;37(21):16430–6.
76. Dalgaard P. Modelling of microbial activity and prediction of shelf life for packed fresh fish. Int J Food Microbiol. 1995;26(3):305–17.
77. Beckers L, Masset J, Hamilton C, Delvigne F, Toye D, Crine MD, et al. Investigation of the links between mass transfer conditions, dissolved hydrogen concentration and biohydrogen production by the pure strain Clostridium butyricum CWBI1009. Biochem Eng J. 2015;98:18–28.
78. Mamimin C, Prasertsan P, Kongjan P, O-Thong S. Effects of volatile fatty acids in biohydrogen effluent on biohythane production from palm oil mill effluent under thermophilic condition. Electron J Biotechnol. 2017;29:78–85.
79. Khanna N, Kotay SM, Jose Gilbert J, Das D. Improvement of biohydrogen production by Enterobacter cloacae IIT-BT 08 under regulated pH. J Biotechnol. 2011;152(1–2):9–15.
80. Song Y, Lu Y, Yu L. Stoichiometry and Thermodynamic Analysis on Biohydrogen Production from Xylose by Klebsiella oxytoca GS-4-08. Energy Fuels. 2019;33(1):356–61.
81. Luxem KE, Nguyen AJ, Zhang X. Biohydrogen production relationship to biomass composition, growth, temperature and nitrogenase isoform in the anaerobic photoheterotrophic diazotroph Rhodopseudomonas palustris. Int J Hydrog Energy. 2022;47(66):28399–409.
82. Zheng G, Kang Z, Qian Y, Wang L. Enhanced biohydrogen generation from organic wastewater containing NH4+ by phototrophic bacteria Rhodobacter sphaeroides AR-3. Front Environ Sci Eng China. 2009;3(4):387–92.
83. Ho K, Chen Y, LEE DJ. Biohydrogen production from cellobiose in phenol and cresol-containing medium using Clostridium sp. R1. Int J Hydrog Energy. 2010;35(19):10239–44.
84. Hsieh P, Lai YC, Chen K, Hung CH. Explore the possible effect of TiO2 and magnetic hematite nanoparticle addition on biohydrogen production by Clostridium pasteurianum based on gene expression measurements. Int J Hydrog Energy. 2016;41(46):21685–91.
85. Dreschke G, Papirio S, Sisinni DMG, Lens PNL, Esposito G. Effect of feed glucose and acetic acid on continuous biohydrogen production by Thermotoga neapolitana. Bioresour Technol. 2019;273:416–24.
86. Ciranna A, Ferrari R, Santala VP, Karp MT. Inhibitory effects of substrate and soluble end products on biohydrogen production of the alkalithermophile Caloramator celer: Kinetic, metabolic and transcription analyses. Int J Hydrog Energy. 2014;39(12):6391–401.
87. Dhar BR, Elbeshbishy E, Nakhla GF. Influence of iron on sulfide inhibition in dark biohydrogen fermentation. Bioresour Technol. 2012;126:123–30.
88. Zheng G, Wang L, Kang Z. Feasibility of biohydrogen production from tofu wastewater with glutamine auxotrophic mutant of Rhodobacter sphaeroides. Renew Energy. 2010;35(12):2910–3.
89. Pakpour F, Mohammadi M, Najafpour-Darzi G. Effect of ferric citrate on biohydrogen production from syngas using rhodopseudomonas palustris PT. Middle East J Sci Res. 2013;14(9):1242–6.
90. Pekgöz G, Gündüz U, Eroılu I, Yücel M, Kovács KL, Ra´khely G. Effect of inactivation of genes involved in ammonium regulation on the biohydrogen production of Rhodobacter capsulatus. Int J Hydrog Energy. 2011;36(21):13536–46.
91. Knutson CM, Plunkett MH, Liming RA, Barney BM. Efforts toward optimization of aerobic biohydrogen reveal details of secondary regulation of biological nitrogen fixation by nitrogenous compounds in Azotobacter vinelandii. Appl Microbiol Biotechnol. 2018;102(23):10315–25.
92. Oh YK, Seol E, Kim J, Park S. Fermentative biohydrogen production by a new chemoheterotrophic bacterium Citrobacter sp. Y19. Int J Hydrog Energy. 2003;28(12):1353–9.
93. Goud RK, Sarkar O, Chiranjeevi P, S. VM. Bioaugmentation of potent acidogenic isolates: A strategy for enhancing biohydrogen production at elevated organic load. Bioresour Technol. 2014;165(C):223–32.